Continuous-Time Discrete-Distribution Theory for Activity-Driven Networks

Lorenzo Zino, Alessandro Rizzo, and Maurizio Porfiri

A continuous-time discrete-distribution theory for activity-driven networks

Lorenzo Zino [1],[*] Alessandro Rizzo [2],[†] and Maurizio Porfiri [3][‡]

[1] *Dipartimento di Scienze Matematiche "G. L. Lagrange", Politecnico di Torino, Torino, Italy*
[2] *Dipartimento di Automatica e Informatica, Politecnico di Torino, Torino, Italy*
[3] *Department of Mechanical and Aerospace Engineering,*
New York University Tandon School of Engineering, Brooklyn NY, USA
(Dated: October 26, 2016)

Activity-driven networks are a powerful paradigm to study epidemic spreading over time-varying networks. Despite significant advances, most of the current understanding relies on discrete-time computer simulations, in which each node is assigned an activity potential from a continuous distribution. Here, we establish a continuous-time discrete-distribution framework toward an analytical treatment of the epidemic spreading, from its onset to the endemic equilibrium. In the thermodynamic limit, we derive a nonlinear dynamical system to accurately model the epidemic spreading and leverage techniques from the fields of differential inclusions and adaptive estimation to inform short- and long-term predictions. We demonstrate our framework through the analysis of two real-world case studies, exemplifying different physical phenomena and time scales.

The study of time-varying networks has greatly contributed to our understanding of epidemic spreading, pushing the state of the art beyond the limitations imposed by time-invariant networks of contacts [1–9]. Activity-driven networks (ADNs) have emerged as a powerful paradigm to model the co-evolution of the network of contacts and the individual dynamics [10–21]. Most of the studies on ADNs are based on extensive Monte Carlo simulations, and analytical results are only limited to linearized mean-field approximations.

Here, we seek to establish an analytical framework to study the entire dynamics of the epidemic spreading at the population level (from the zero-infected condition to the endemic equilibrium). Differently from the original ADN formulation, where a discrete-time epidemic model is implemented with a continuous probability distribution for the nodes' activities, we formulate a continuous-time model with a discrete distribution. This change of perspective leads to a rigorous analytical treatment, without the need of extensive Monte Carlo simulations that have constituted the primary tool for the study of ADNs. Our approach is not prone to the confounds associated with the selection of the time step, which has been proven to influence the dynamics of the discrete-time dynamical process [22]. Our theory relies on a reduced number of parameters with respect to traditional ADNs [10–20]. This is critical for robust parameter identification from real-world data [15, 23–26].

We consider a (large) population of n individuals, each associated with a node of a time-varying undirected graph $\mathcal{G}(t) = (\mathcal{V}, \mathcal{E}(t))$, with $t \in \mathbb{R}^+$. $\mathcal{V} = \{1, \ldots, n\}$ is the node set and $\mathcal{E}(t)$ is the time-varying edge set, which is related to the network of contacts. We focus on a susceptible-infected-susceptible process [27]. Each node $v \in \mathcal{V}$ is assigned a time-invariant activity rate a_v, which represents the expected number of contacts that node v generates in a unit time interval. Starting from $t = 0$, node v becomes active after a time that is sampled from an exponentially distributed random variable with parameter a_v [28]. When a node activates, it contacts exactly one node uniformly at random in $\mathcal{V}$, generating a single edge. If this edge connects an infected node with a susceptible one, then the epidemics propagates with a fixed probability λ, otherwise nothing happens. We suppose that the duration of the contact is instantaneous, so that λ is considered a per-contact infection probability. The edge is instantaneously removed, and the node may activate again according to the same rule. Each infected node recovers after a time that is drawn from an exponentially distributed random variable with parameter μ, becoming susceptible again. Thus, μ^{-1} is the expected time needed by an individual to recover [29].

The proposed discrete activity distribution follows a power-law with k equidistant activation classes, characterized by an activity rate a_i ($a_1 < \cdots < a_k$). For the generic i-th class, we denote with n_i its number of nodes and we let $n_i \propto a_i^{-\gamma}$. The parameter γ controls the heterogeneity among individuals, similar to the classical ADN paradigm with a continuous distribution of activity potentials [30].

We indicate with $Y_v(t) \in \{S, I\}$ the state of node v at time t, which can be either susceptible (S) or infected (I), and we assemble all the states in a vector $Y(t) \in \{S, I\}^{\mathcal{V}}$. Towards analyzing the epidemic spreading at the population level, we map $Y(t)$ to a k-dimensional stochastic process $Z(t) := Z[Y(t)]$, encapsulating the fraction of infected nodes in each activation class. The i-th compo-

[*] Also at Dipartimento di Matematica "G. Peano", Università degli Studi di Torino, Torino, Italy.
[†] Also at Office of Innovation, New York University Tandon School of Engineering, Brooklyn NY, USA; alessandro.rizzo@polito.it
[‡] mporfiri@nyu.edu

nent, $Z_i(t)$, is the fraction of infected nodes with activity rate a_i, at time t.

In the thermodynamic limit $n \to \infty$, the fraction of nodes $(n_1/n, \ldots, n_k/n)$ in each of the activation classes converges to $(\eta_1, \ldots, \eta_k)$, independent of n, due to the central limit theorem. Then, Kurtz' theorem [31] ensures that for every finite time horizon, the stochastic process $Z(t)$ is close to a deterministic dynamical system with vector variable $\zeta(t)$, solution of the following set of ordinary differential equations (ODEs):

$$\dot{\zeta}_i = -\mu\zeta_i + \lambda(1 - \zeta_i)(a_i x_1 + x_2), \quad (1)$$

with $i = 1, \ldots, k$ and $\zeta_i(0) = Z_i(0)$. Here, the macroscopic variable $x_1 = \sum \eta_h \zeta_h$ represents the fraction of infected individuals across all classes, which is the main observable in the study of epidemic spreading. The macroscopic variable $x_2 = \sum \eta_h a_h \zeta_h$ takes into consideration the fraction of infected nodes weighted by their individual activity rates. In general, we define $x_j = \sum \eta_h a_h^{j-1} \zeta_h$; Table I summarizes our notation.

From (1), we appreciate that the drift in the fraction of infected nodes in each class is determined by three effects: the recovery of infected nodes $(-\mu\zeta_i)$; the spreading associated with active nodes in the i-th class generating contacts toward infected nodes $(\lambda(1 - \zeta_i)a_i x_1)$; and the spreading related to active infected nodes generating contacts with the nodes of the i-th class $(\lambda(1 - \zeta_i)x_2)$.

The elegant form of the system dynamics (1) in terms of the variables $\zeta_1, \ldots, \zeta_k$ lends itself into rigorous and revealing schemes to gain insight into the physics of the epidemic spreading. Here, we focus on two complementary strategies that could be systematically utilized for short- and long- term predictions. First, we propose the use of differential inclusions to establish rigorous bounds for the transient and endemic equilibrium of the system. Second, we explore the integration of estimation techniques to accurately predict the population of infected individuals from sporadic data which could be collected in real-world scenarios.

Integrating (1) allows to closely simulate the epidemic spreading without the need of Monte Carlo simulations. To verify this claim and demonstrate the correspondence between continuous- and discrete-time epidemic models, we consider two different dynamics on real-world phenomena, modeled through ADNs: flu spreading in a uni-

FIG. 1: Time evolution of the fraction of infected nodes for the flu (a) and Twitter (b) case studies. Comparison between discrete-time continuous-distribution ADN process (blue, dashed), our continuous-time discrete-distribution approach (green, dotted) model, and theoretical predictions (red, solid) from (1).

versity campus and trend diffusion on Twitter. System parameters are obtained from case studies [10, 32–35], as detailed in the supplementary material, and are summarized in Table II. We compare the outcome of Monte Carlo simulations averaged over 200 trials for both the continuous- and the discrete-time processes, along with the integration of the deterministic system (1). In both examples, the activity distribution is discretized over $k = 59$ equidistant activation classes. Fig. 1 demonstrates the equivalence of our approach with respect to traditional ADNs in Monte Carlo simulations, along with the validity of equation (1) to exactly predict the epidemic spreading.

To facilitate the mathematical treatment of the k-dimensional system (1), we rewrite the system dynamics in terms of the first k macroscopic variables, $x_1, \ldots, x_k$. Through this change of variables, the epidemic spreading is governed by the following ODEs:

$$\begin{cases} \dot{x}_1 = (\lambda\alpha_1 - \mu)x_1 + \lambda x_2 - 2\lambda x_1 x_2, \\ \dot{x}_2 = \lambda\alpha_2 x_1 + (\lambda\alpha_1 - \mu)x_2 - \lambda x_1 x_3 - \lambda x_2^2, \\ \dot{x}_3 = \lambda\alpha_3 x_1 + \lambda\alpha_2 x_2 - \mu x_3 - \lambda x_1 x_4 - \lambda x_2 x_3, \\ \ldots \\ \dot{x}_k = \lambda\alpha_k x_1 + \lambda\alpha_{k-1}x_2 - \mu x_k - \lambda x_1 \sum \eta_h a_h^k \zeta_h - \lambda x_2 x_k, \end{cases} \quad (2)$$

where $\alpha_j = \sum \eta_h a_h^j$ are the moments of the activity rates distribution, whose first two values are also reported in

TABLE I: Notation.

k	number of activation classes
a_i	activation rate of nodes in the i-th class
η_i	fraction of nodes in the i-th class
λ	per-contact infection probability
μ	recovery rate
ζ_i	fraction of infected nodes in the i-th class
x_j	macroscopic variables, $x_j = \sum \eta_h a_h^{j-1} \zeta_h$
α_j	j-th moment of the distribution α, $\alpha_j = \sum \eta_h a_h^j$

TABLE II: Parameters of real-world case studies based on ADNs.

Parameter	flu	Twitter
n	30896	531788
k	59	59
γ	2.09	2.10
λ	0.430	0.332
μ	0.138	0.0997
α_1	0.317	0.536
α_2	0.381	0.781
time unit	day	minute

Table II for completeness. This system is well-posed since the term $\sum \eta_h a_h^k \zeta_h$ in the k-th equation is a linear combination of the linearly independent variables $x_1, \ldots, x_k$.

The study of (2) offers important insight on the epidemic spreading, beyond the mere computation of the epidemic threshold $(\alpha_1 + \sqrt{\alpha_2})^{-1}$ from linear stability analysis [10–12]; details are presented in the supplementary material. However, numerical instabilities may emerge when considering power-laws with $\gamma \in [2,3]$, where all statistical moments from the second onwards may blow up. Moreover, prescribing initial conditions for higher order macroscopic variables beyond x_1 may be not feasible when dealing with experimental data.

A possible approach to address these issues is to project the k-dimensional dynamics to a lower dimensional space consisting of only $k^* \ll k$ equations. We approximate the term x_{k^*+1} using two elementary bounds: $a_1 x_{k^*} \leq x_{k^*+1} \leq a_k x_{k^*}$ and $x_{k^*+1} \leq \alpha_{k^*}$. Using these bounds, we can reduce system of k ODEs in (2) to a system of k^* ordinary differential inclusions (ODIs) [36], consisting of one inclusion and $k^* - 1$ equations.

If $k^* = 1$, we bound $a_1 x_1 \leq x_2 \leq \min\{\alpha_1, a_k x_1\}$, reducing (2) to a single ODI. This one-dimensional system should not be contemplated to accurately predict the evolution of the process during the transient, between the zero-infected condition and the endemic equilibrium, due to the conservativeness of the bounds during such a transient phase. However, it can be effectively used to analytically determine an interval $\mathcal{I}$ for the endemic equilibrium $\bar{x}_1$, which is

$$\left[\max\left\{ \frac{\lambda\alpha_1}{\lambda\alpha_1 + \mu}, \frac{\lambda(a_k + \alpha_1) - \mu}{2\lambda a_k} \right\}, \frac{\lambda(a_1 + \alpha_1) - \mu}{2\lambda a_1} \right],$$
(3a)

if $\lambda\alpha_1 > \mu$, and

$$\left[\frac{\lambda(a_1 + \alpha_1) - \mu}{2\lambda a_1}, \min\left\{ \frac{\lambda\alpha_1}{\lambda\alpha_1 + \mu}, \frac{\lambda(a_k + \alpha_1) - \mu}{2\lambda a_1} \right\} \right],$$
(3b)

if $\lambda\alpha_1 < \mu$. Notice that, if $\lambda\alpha_1 = \mu$, we analytically compute $\bar{x}_1 = 1/2$.

To demonstrate the use of these bounds we refer, here and henceforth, to the two real-world case studies on flu spreading and trend diffusion on Twitter. From simulations in Fig. 2, we evince that the accuracy of the bounds depends on the system parameters. Specifically, our results suggest that the closer is the endemic state to $\bar{x}_1 = 1/2$ (that is, $\alpha_1 \lambda = \mu$), the more precise the bounds are.

An improved prediction of the transient phase is obtained with $k^* = 2$, which leads to an ODI for the evolution of x_2, coupled to the first ODE in (2). As detailed in the supplementary material, we establish the two fol-
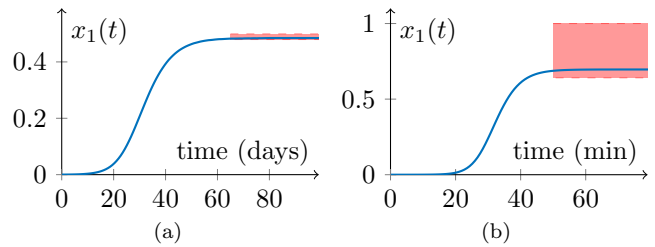
FIG. 2: Averaged Monte Carlo simulations of a discrete-time continuous-distribution ADN process (blue) and theoretical bounds on the endemic equilibrium state (computed for $k^* = 1$, in red), for flu (a) and Twitter (b) case studies. From Table II, $\alpha_1 \lambda / \mu$ is equal to 0.988 in (a) and 1.785 in (b).

lowing ancillary ODEs:

$$\dot{x}_2 = \lambda(\alpha_2 - \phi_{\varepsilon,x_2}(x_1))x_1 + (\lambda\alpha_1 - \mu)x_2 - \lambda x_2^2,$$
(4a)

$$\dot{x}_2 = \lambda(\alpha_2 - \phi_{\varepsilon,x_2}(1 - x_1))x_1 + (\lambda\alpha_1 - \mu)x_2 - \lambda x_2^2,$$
(4b)

where $\phi_{\varepsilon,x_2}(x_1)$, is a continuous function that, in the limit $\varepsilon \to 0$, tends to the Heaviside function

$$\phi_{\varepsilon,x_2}(x_1) \to \begin{cases} a_1 x_2 & \text{if } x_1 < 1/2, \\ \min\{a_k x_2, \alpha_2\} & \text{if } x_1 > 1/2. \end{cases}$$
(5)

The upper- and lower-bounds for x_1 are obtained by coupling the first ODE in (2) with (4a) and (4b), and integrating in the limit as $\varepsilon \to 0$. Simulation results in Fig. 3 demonstrate the accuracy of the bounds in capturing the transient response. Higher endemic equilibria seem manifest into tighter prediction bounds during the transient, albeit the upper bound becomes conservative as time progresses. In general, the predictions of the endemic state from $k^* = 2$ are less precise than the simpler closed-form results for $k^* = 1$. This is related to the solutions of the ancillary ODEs (4a) and (4b) leaving the bounds for $k^* = 1$. With this in mind, the overall predic-
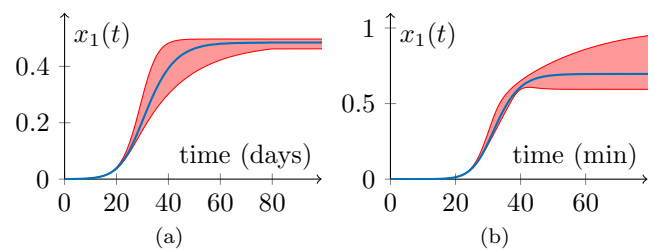
FIG. 3: Averaged Monte Carlo simulations of a discrete-time continuous-distribution ADN process (blue) and theoretical bounds on the dynamics of the epidemic spreading (computed for $k^* = 2$ with $\varepsilon = 10^{-3}$, in red), for flu (a) and Twitter (b) case studies.

tion accuracy could be improved combining the bounds in Figs. 2 and 3.

An alternative strategy for the analysis of system (2) entails the use of epidemic data, sampled at the population level at a time period T, to drive the reduction of the dynamics on a lower dimensional space. Given the accuracy of (4) in estimating the transient response of the system, we focus on a two-dimensional dynamics in terms of x_1 and x_2. With reference to (2), we consider only the first two ODEs and we hypothesize that x_3 is linear in x_1 with a proportionality constant C that is estimated from epidemic data. Specifically, we propose the following two-dimensional dynamics:

$$
\begin{cases}
\dot{x}_1 = -\mu x_1 + \lambda \alpha_1 x_1 + \lambda x_2 - 2\lambda x_1 x_2, \\
\dot{x}_2 = \lambda \alpha_2 x_1 + (\lambda \alpha_1 - \mu) x_2 - \lambda C x_1^2 - \lambda x_2^2.
\end{cases}
\tag{6}
$$

As a first approximation, we hypothesize that C is constant throughout the entire epidemic spreading and set to $C = \alpha_2$, which corresponds to a homogeneous distribution of infected individuals over all the activation classes. Our prediction of the infected population is defined piece-wise in time. In particular, we we denote the piece-wise predictions with $x_1^{(h)}(t)$ and $x_2^{(h)}(t)$, in the interval $t \in [hT, hT + T)$ [37, 38], where $h \in \mathbb{Z}^+$. These predictions are informed by the knowledge of the overall infected fraction of population X_{hT} at the sampling times hT. We initialize the algorithm at time $t = 0$ by setting $x_1^{(0)}(0) = X_0$ and $x_2^{(0)}(0) = X_0 \alpha_1$. The algorithm runs through the following steps: i) system (6) is integrated from hT to $(h+1)T$, producing the solutions $x_1^{(h)}(t)$ and $x_2^{(h)}(t)$; ii) at $t = (h+1)T$, the initial conditions for marching in time are set as $x_1^{(h+1)}(t) = X_{(h+1)T}$ and $x_2^{(h+1)}(t) = x_2^{(h)}(t)$; and iii) h is incremented by 1 and the process resumes to step i).

This algorithm is only based on the fraction of infected nodes at the inception of each time window of duration T, which is central for real-world applications. For example, it may be possible to periodically estimate the number of individuals affected by flu or the number of mentions and re-tweets of a specific trend. The knowledge of the detailed state of all the network nodes is not required by the algorithm, which dispenses with information about higher order microscopic variables. In Fig. 4, we demonstrate the use of the prediction algorithm against a simulation for the flu case study, by using a time window of a day or a week. Short-term forecasts (daily) are very close to the real dynamics (the average error is less than 1%), while forecasts on longer horizons (weekly) tend to be less accurate (with an average error around 10%).

To improve on the finite horizon forecast algorithm, we may treat C as piece-wise constant in time and adaptively update it during each prediction window. We initiate the algorithm by setting $C_0 = \alpha_2$. Then, fixing a real constant $\beta > 0$, at the end of each iteration, C_h is updated

(a) Daily forecasts

(b) Weekly forecasts

(c) Daily forecasts

(d) Weekly forecasts
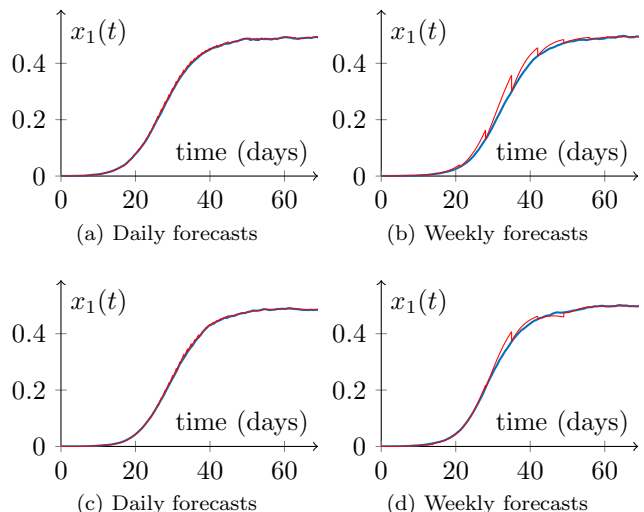
FIG. 4: Simulation of a discrete-time continuous-distribution ADN (blue), for the flu case study, and our predictions over a finite time horizon of one day and one week (red). Predictions in (a) and (b) are obtained with a constant estimate for C, while those in (c) and (d) are based on the on-line adaptive update in (7) with $\beta = 1$. A similar result for the Twitter case study is presented in the supplementary material.

as [37, 38]

$$
C_{h+1} = C_h \left(1 + \beta \frac{X_{(h+1)T} - x_1^{(h)}((h+1)T)}{1 - 2X_{(h+1)T}} \right).
\tag{7}
$$

Here, C is incremented by a term that is proportional to the prediction error at the inception of a new prediction window. The effect of the denominator is to change the sign of the increment when $X_{(h+1)T} > 1/2$, following a line of reasoning similar to the one used to define $\phi_{\varepsilon, x_2}(x_1)$ in (5). In Fig. 4, we demonstrate the improvement of the approach, which is successful in closely predicting population level dynamics even with only data available on a weekly basis.

In summary, we have proposed a new framework to study epidemic spreading over ADNs. While intuition may conceive epidemic models to be executed in discrete-time on nodes whose activity is drawn from a continuous distribution, our approach posits a different view. By discretizing the activity distribution and considering a continuous-time evolution, we put forward a mathematically tractable approach to study epidemic spreading from its onset to the endemic equilibrium. In the thermodynamic limit, we have shown that epidemic spreading can be described through a set of coupled ODEs. Techniques from the field of differential inclusions were leveraged to gather insight on the transient response and endemic equilibrium. Toward connecting the theoretical framework with real data, we introduced an adaptive es-

timation technique that affords the accurate prediction of the epidemics from coarse information only seldom acquired. Although we specialized the treatment to SIS processes, the framework could be extended to other processes over ADNs [10–21], by tailoring the individual dynamics.

Our continuous-time discrete-distribution framework offers a rigorous mathematical basis for overcoming some of the limitations of the ADN paradigm. For example, the treatment of non-exponential inter-event times may be tackled by modifying the ODE system (1) to incorporate specific statistical properties of the inter-event times distribution [39]. Non mean-field dynamics may be studied by partitioning the nodes in several classes of activation, differentiating the probability of contagion within each class and between different classes.

[1] M. Frasca, A. Buscarino, A. Rizzo, L. Fortuna, and S. Boccaletti, Phys. Rev. E **74**, 036110 (2006).
[2] E. Volz and L. A. Meyers, J. R. Soc. Int. **6**, 233 (2008).
[3] P. Holme and J. Saramäki, Phys. Rep. **519**, 97 (2012).
[4] R. Pastor-Satorras, C. Castellano, P. Van Mieghem, and A. Vespignani, Rev. Mod. Phys. **87**, 925 (2015).
[5] E. Valdano, L. Ferreri, C. Poletto, and V. Colizza, Phys. Rev. X **5**, 021005 (2015).
[6] M. Ogura and V. M. Preciado, IEEE Trans. Netw. Sci. Eng. **3**, 44 (2016).
[7] C. Vestergaard, E. Valdano, M. Génois, C. Poletto, V. Colizza, and A. Barrat, Eur. J. of Appl. Math. , 1 (2016).
[8] A. Koher, H. Lentz, P. Hövel, and I. Sokolov, PLOS One **11**, e0151209 (2016).
[9] A. Braunstein and A. Ingrosso, Sci. Rep. **6**, 27538 (2016).
[10] N. Perra, B. Gonçalves, R. Pastor-Satorras, and A. Vespignani, Sci. Rep. **2**, 469 (2012).
[11] S. Liu, N. Perra, M. Karsai, and A. Vespignani, Phys. Rev. Lett. **112**, 118702 (2014).
[12] A. Rizzo, M. Frasca, and M. Porfiri, Phys. Rev. E **90**, 042801 (2014).
[13] M. Starnini and R. Pastor-Satorras, Phys. Rev. E **89**, 032807 (2014).
[14] K. Sun, A. Baronchelli, and N. Perra, EPJ B **88**, 1 (2015).
[15] A. Rizzo, B. Pedalino, and M. Porfiri, J. Theor. Biol. **394**, 212 (2016).
[16] Y. Lei, X. Jiang, Q. Guo, Y. Ma, M. Li, and Z. Zheng, Phys. Rev. E **93**, 032308 (2016).
[17] C. Liu, L.-X. Zhou, C.-J. Fan, L.-A. Huo, and Z.-W. Tian, Phys. A **432**, 269 (2015).
[18] M.-X. Liu, W. Wang, Y. Liu, M. Tang, S.-M. Cai, and H.-F. Zhang, arXiv preprint arXiv:1605.04557 (2016).
[19] A. Rizzo and M. Porfiri, EPJ B **89**, 1 (2016).
[20] Y. Zou, W. Deng, W. Li, and X. Cai, Int. J. Mod. Phys. C , 1650090 (2016).
[21] T. Aoki, L. E. C. Rocha, and T. Gross, Phys. Rev. E **93**, 040301 (2016).
[22] B. Ribeiro, N. Perra, and A. Baronchelli, Sci. Rep. **3**, 3006 (2013), 1211.7052.
[23] M. Ajelli, B. Gonçalves, D. Balcan, V. Colizza, H. Hu, J. Ramasco, S. Merler, and A. Vespignani, BMC Inf. Dis. **10**, 190 (2010).
[24] P. Bajardi, C. Poletto, J. Ramasco, M. Tizzoni, V. Colizza, and A. Vespignani, PLOS One **6**, e16591 (2011).
[25] M. Gomes, A. Pastore, L. Rossi, D. Chao, I. Longini, M. Halloran, and A. Vespignani, PLOS Cur. Out. , 1 (2014).
[26] S. Merler, M. Ajelli, L. Fumanelli, M. Gomes, A. Piontti, L. Rossi, D. Chao, I. Longini, M. Halloran, and A. Vespignani, The Lancet Inf. Dis. **3099**, 1 (2015).
[27] F. Brauer and C. Castillo-Chavez, *Mathematical Models in Population Biology and Epidemiology* (Springer, New York, NY, 2011).
[28] I. Olkin, L. Gleser, and C. Derman, *Probability Models and Applications* (Prentice Hall, Upper Saddle River, NJ, 1994).
[29] The relationship with discrete-time ADN models is straightforward. In a time step Δt, the continuous-time model establishes as many edges as in a realization of the discrete-time model. The activity rate of a node in continuous-time corresponds to the product of its activity potential and the number of contacts it can establish in the time step. The probability that an infected node recovers in a discrete-time step is $1 - e^{-\mu \Delta t}$. The per-contact infection probability does not change between continuous- and discrete-time.
[30] The original formulation of ADNs posits a continuous power-law distribution with $2 \leq \gamma \leq 3$.
[31] T. G. Kurtz, *Approximation of Population Processes*, Vol. 36 (SIAM, Philadelphia, PA, 1981).
[32] L. Kim, M. Abramson, K. Drakopoulos, S. Kolitz, and A. Ozdaglar, "Estimating social network structure and propagation dynamics for an infectious disease," in *Social Computing, Behavioral-Cultural Modeling and Prediction: 7th International Conference, SBP 2014, Washington, DC, USA, April 1-4, 2014. Proceedings*, edited by W. G. Kennedy, N. Agarwal, and S. J. Yang (Springer International Publishing, Cham, 2014) pp. 85–93.
[33] K. Zhao and G. Bianconi, Front. in Phys. **2**, 1 (2011).
[34] J. Skaza and B. Blais, Phys. A **465**, 289 (2017).
[35] W. Aiello, F. Chung, and L. Lu, in *Proceedings of the 32nd Annual ACM Symposium on Theory of Computing*, STOC '00 (ACM, New York, NY, USA, 2000) pp. 171–180.
[36] J.-P. Aubin and A. Cellina, *Differential Inclusions: Set-Valued Maps and Viability Theory*, Vol. 264 (Springer, New York, NY, 2012).
[37] G. Tao, *Adaptive Control Design and Analysis*, Vol. 37 (John Wiley & Sons, New York, NY, 2003).
[38] L. Grüne and J. Pannek, *Nonlinear Model Predictive Control* (Springer, New York, NY, 2011).
[39] J. Delvenne, R. Lambiotte, and L. E. C. Rocha, Nature Commun. **6** (2015).